Video Article

Synthesis and Reaction Chemistry of Nanosize Monosodium Titanate

Mark C. Elvington[1], Kathryn M. L. Taylor-Pashow[2], Michael H. Tosten[2], David T. Hobbs[2]

[1]Savannah River Consulting, L.L.C.

[2]Savannah River National Laboratory

Correspondence to: Kathryn M. L. Taylor-Pashow at Kathryn.Taylor-Pashow@srnl.doe.gov

URL: https://www.jove.com/video/53248
DOI: doi:10.3791/53248

Keywords: Chemistry, Issue 108, Nanoparticles, sol-gel, titanate, surfactant, ion exchange, hydrogen peroxide

Date Published: 2/23/2016

Citation: Elvington, M.C., Taylor-Pashow, K.M., Tosten, M.H., Hobbs, D.T. Synthesis and Reaction Chemistry of Nanosize Monosodium Titanate. *J. Vis. Exp.* (108), e53248, doi:10.3791/53248 (2016).

Abstract

This paper describes the synthesis and peroxide-modification of nanosize monosodium titanate (nMST), along with an ion-exchange reaction to load the material with Au(III) ions. The synthesis method was derived from a sol-gel process used to produce micron-sized monosodium titanate (MST), with several key modifications, including altering reagent concentrations, omitting a particle seed step, and introducing a non-ionic surfactant to facilitate control of particle formation and growth. The resultant nMST material exhibits spherical-shaped particle morphology with a monodisperse distribution of particle diameters in the range from 100 to 150 nm. The nMST material was found to have a Brunauer-Emmett-Teller (BET) surface area of 285 m^2g^{-1}, which is more than an order of magnitude higher than the micron-sized MST. The isoelectric point of the nMST measured 3.34 pH units, which is a pH unit lower than that measured for the micron-size MST. The nMST material was found to serve as an effective ion exchanger under weakly acidic conditions for the preparation of an Au(III)-exchange nanotitanate. In addition, the formation of the corresponding peroxotitanate was demonstrated by reaction of the nMST with hydrogen peroxide.

Video Link

The video component of this article can be found at https://www.jove.com/video/53248/

Introduction

Titanium dioxide and alkali metal titanates are widely used in a variety of applications such as pigments in paint and skin care products and as photocatalysts in energy conversion and utilization.[1-3] Sodium titanates have been shown to be effective materials to remove a range of cations over a wide range of pH conditions through cation exchange reactions.[4-7]

In addition to the applications just described, micron-sized sodium titanates and sodium peroxotitanates have recently been shown to also serve as a therapeutic metal delivery platform. In this application, therapeutic metal ions such as Au(III), Au(I), and Pt(II) are exchanged for the sodium ions of monosodium titanate (MST). *In vitro* tests with the noble metal-exchanged titanates indicate suppression of the growth of cancer and bacterial cells by an unknown mechanism.[8,9]

Historically, sodium titanates have been produced using both sol-gel and hydrothermal synthetic techniques resulting in fine powders with particle sizes ranging from a few to several hundred microns.[4,5,10,11] More recently, synthetic methods have been reported that produced nanosize titanium dioxide, metal-doped titanium oxides, and a variety of other metal titanates. Examples include sodium titanium oxide nanotubes (NaTONT) or nanowires by reaction of titanium dioxide in excess sodium hydroxide at elevated temperature and pressure,[12-14] sodium titanate nanofibers by reaction of peroxotitanic acid with excess sodium hydroxide at elevated temperature and pressure,[15] and sodium and cesium titanate nanofibers by delamination of acid-exchanged micron-sized titanates.[16]

The synthesis of nanosize sodium titanates and sodium peroxotitanates is of interest to enhance ion exchange kinetics, which are typically controlled by film diffusion or intraparticle diffusion. These mechanisms are largely controlled by the particle size of the ion exchanger. In addition, as a therapeutic metal delivery platform, the particle size of the titanate material would be expected to significantly affect the nature of the interaction between the metal-exchanged titanate and the cancer and bacterial cells. For example, bacterial cells, which are typically on the order of 0.5 – 2 µm, would likely have different interactions with micron size particles versus nanosized particles. In addition, non-phagocytic eukaryotic cells have been shown to only internalize particles with a size of less than 1 micron.[17] Thus, the synthesis of nanosize sodium titanates is also of interest to facilitate metal delivery and cellular uptake from the titanate delivery platform. Reducing the size of sodium titanates and peroxotitanates will also increase the effective capacity in metal ion separations and enhance photochemical properties of the material.[16,18] This paper describes a protocol developed to synthesize nanosize monosodium titanate (nMST) under mild sol-gel conditions.[19] The preparation of the corresponding peroxide modified nMST; along with an ion-exchange reaction to load the nMST with Au(III) are also described.

Protocol

1. Synthesis of Nano-monosodium Titanate (nMST)

1. Prepare 10 ml of solution #1 by adding 0.58 ml of 25 wt % sodium methoxide solution to 7.62 ml of isopropanol followed by 1.8 ml of titanium isopropoxide.
2. Prepare 10 ml of solution #2 by adding 0.24 ml of ultrapure water to 9.76 ml of isopropanol.
3. Add 280 ml of isopropanol to a 3-neck 500-ml round bottom flask, followed by 0.44 ml of Triton X-100 (average MW: 625 g/mol). Stir the solution well with a magnetic stir bar.
4. Prepare a dual channel syringe pump to deliver solutions #1 and #2 at a rate of 0.333 ml/min.
5. Load solutions #1 and #2 into two separate 10-ml syringes fitted with a length of tubing that will allow delivery of the solution from the syringe pump to below the solution level in the 500-ml round bottom flask.
6. While stirring, add all of solutions #1 and #2 (10 ml each) to the reaction using the syringe pump programmed in step 1.4.
7. After the addition is complete, cap the flask and continue to stir for 24 hr at RT.
8. Uncap the flask and heat the reaction mixture to ~82 °C (refluxing isopropanol) for 45-90 min, followed by purging with nitrogen while maintaining heating. As isopropanol is evaporated, add ultrapure water intermittently to replace the evaporated isopropanol.
9. After most of the isopropanol has evaporated and the volume of water added is approximately 50 ml, remove the heat and allow the reaction mixture to cool.
10. Collect the product by filtering through a 0.1-µm nylon filter paper, and wash several times with water to remove the surfactant and any residual isopropanol. Do not filter to dryness. After washing is complete, transfer the slurry from the filter into a pre-weighed bottle or vial, and store as an aqueous slurry.
11. Determine the yield by determining the weight percent solids of the slurry. This can be done by measuring the weight of an aliquot of the slurry before and after drying.

2. Au(III) Ion Exchange

1. Transfer 6.50 g of 4.23 wt % nMST slurry to a 50-ml centrifuge tube. This amount may vary based on the actual weight percent of the nMST slurry produced in step 1.10 above, and determined in step 1.11.
2. Weigh out 0.0659 g of $HAuCl_4 \cdot 3H_2O$ into a 1-dram glass vial. The target Ti:Au mass ratio is 4:1.
3. Dissolve the $HAuCl_4 \cdot 3H_2O$ in ~ 1 ml of water, then transfer to the centrifuge tube containing the nMST. Rinse the vial several times with additional water to ensure all of the $HAuCl_4 \cdot 3H_2O$ is transferred to the centrifuge tube containing the nMST.
4. Dilute the suspension with additional water, as necessary, to bring the total volume to 11 ml. Target a final Au(III) concentration of approximately 15 mM.
5. Wrap the centrifuge tube in foil to keep the suspension in the dark, and then tumble the suspension on a shaker rotisserie for a minimum of 4 days.
6. Collect the product by centrifuging at 3,000 x g for 15 min to isolate the solids. Wash the solids three times with distilled water by redispersing in water, and reisolate by centrifuging at 3,000 x g for 15 min to remove any unexchanged Au(III).
7. Store the final product either as an aqueous suspension by redispersing in water, or as a moist solid by decanting off the final wash water and capping the tube. Store the product in the dark.

3. Preparation of the Peroxotitanate

1. Transfer 5 g of a 9.8 wt % slurry of nMST to a small flask.
2. Weigh out 0.154 g of 30 wt % H_2O_2 solution. The target H_2O_2:Ti molar ratio is 0.25:1.
3. While stirring the nMST suspension well add the 0.154 g of H_2O_2 solution drop-wise. Upon H_2O_2 addition, the suspension of white solids immediately turns yellow.
4. After the addition is complete stir the reaction at ambient temperature for 24 hr.
5. Collect the product by filtering through a 0.1-µm nylon filter, and wash several times with water to remove any unreacted H_2O_2. Do not filter to dryness. After washing is complete, transfer the slurry from the filter into a pre-weighed bottle or vial, and store as an aqueous slurry.

Representative Results

MST is synthesized using a sol-gel method in which tetraisopropoxytitanium(IV) (TIPT), sodium methoxide, and water are combined and reacted in isopropanol to form seed particles of MST.[4] Micron-sized particles are then grown by controlled addition of additional quantities of the reagents. The resultant particles feature an amorphous core and an outer fibrous region having dimensions of about 10 nm wide by 50 nm in length.[20]

Figure 1A shows a typical particle size distribution, as measured by dynamic light scattering (DLS), for micron-sized MST prepared using the established sol-gel method. This synthesis produces a multimodal distribution of particles, with the majority around 1 µm. Initial attempts to reduce the particle size of the MST investigated eliminating the seed step and using much more dilute reagent concentrations. In the diluted reaction the final solvent:TIPT volume ratio was 165 compared to 5.14 in the micron-sized MST synthesis, representing a reagent dilution of ~32 during the synthesis. As seen in **Figure 1B**, this resulted in a bimodal distribution with particle sizes centered at 50-100 nm and at 500 nm after 24 hr of reaction. After 48 hr, a trimodal distribution is observed with the appearance of particles measuring 1,000 nm (1 µm) in size (**Figure 1C**). DLS measurements at shorter reaction times show a bimodal distribution of particle sizes similar to that shown in **Figure 1B** except the

distribution is centered at smaller particle sizes. Thus, we conclude that the reduced reagent concentration and absence of the seed step leads to smaller particles produced initially, but particle growth continues resulting in a mixture of both nano and micron-sized MST.

Over the last decade there have been a number of papers reporting the addition of surfactants in sol–gel syntheses to control particle size resulting in the production of nanosize titanium dioxide, metal-doped titanium dioxides and multi-metal titanium oxides.[21-26] Based on these findings, we initiated a series of tests to determine if the addition of surfactant to the MST synthesis would control particle growth allowing the sole production of nanosize particles. A number of non-ionic surfactants (Brig 52; Merpol A; Triton X series (X-15, X-45, X-100, X-165, X-405); TWEEN 20; 2,4,7,9-tetramethyl-5-decyne-4,7-diol ethoxylate; and Zonyl FS300) as well as one anionic surfactant (sodium docusate) and one cationic surfactant (CTAB) were screened.

Initial experiments screened surfactants at a concentration of 0.12 moles of surfactant per mole of TIPT. Products from these reactions were screened using DLS for polydispersity and average particle size. Triton X-100, Triton X-165, Brij 52, and Zonyl FS300 showed a good combination of small particle size (Z_{ave} < 150 nm) and monodispersity, with Triton X-100 and Triton X-165 showing the most narrow range of particle sizes. Additional experiments were then performed to examine a range of surfactant concentrations from 0.012 to 1.2 moles of surfactant per mole of TIPT. Higher surfactant concentrations resulted in broader distributions of particle sizes, while lower concentrations resulted in bimodal distributions suggesting that there was insufficient surfactant to limit the growth of particles. Triton X-100 at 0.12 moles per mole of TIPT appeared close to optimal for the synthesis of uniform nMST particles (**Figures 2** and **3**).

Temperature plays a key role in the conversion of the product from a gel to particulate form. Transmission electron microscopy (TEM) images before and after heating to 82 °C show the product appears as a semi-particulate/semi-gel-like state prior to heating, but after heating the product appears solid and particulate in nature. Thus, the low temperature heating for 45-90 min is needed to complete particulate formation of the nMST.

Additional characterization of the nMST included determination of surface area and isoelectric point (IEP). Surface area measurements were obtained by Brunauer-Emmett-Teller (BET) analysis of nitrogen absorption isotherms. The BET surface area measured 285 m^2g^{-1} for the nMST compared to only 20 m^2g^{-1} for the micron-sized MST. The higher surface area for the nMST is consistent with the much smaller particle size of the nMST. Zeta potential measurements were performed over a range of pH conditions to determine the IEP for the nano and microtitanates. The IEPs determined are as follows: nMST = 3.34; peroxide-modified nMST = 2.05; MST = 4.46; peroxide-modified MST = 3.43. The nMST exhibited a lower IEP than MST indicating a higher fraction of surface sites available for protonation. This would be expected given the order of magnitude higher surface area of the nMST. Conversion of the nMST to the peroxide-modified nMST form lowered the IEP by more than a pH unit. A similar trend was observed upon conversion of MST to the peroxo form. The lower IEP for the peroxide-modified nMST and peroxide-modified MST materials likely results from the presence of non-bridging peroxo species that can be easily protonated and deprotonated.

The success of the surface modification of the nMST by H_2O_2 can be immediately observed from the color change from white to yellow. This color change is due to the η^2-bound protonated hydroperoxo-titanium ligand-to-metal-charge-transfer absorption band at 385 nm.[27,28] Fourier transform infrared spectroscopy (FT-IR) also confirmed the formation of the peroxotitanate species as evidenced by the appearance of an absorption band at 883 cm^{-1} for the peroxide modified nMST (**Figure 4**) which is absent in the untreated nMST material. This band is very near the region of 845-875 cm^{-1} that is reported for the O-O stretching vibration in peroxides.[29] TEM and scanning electron microscopy (SEM) analyses indicated that the particle size and morphology were retained after the peroxide reaction.

To determine the extent of the Au(III) ion-exchange, samples of the Au(III)-loaded solids were digested in hot nitric acid, followed by analysis of the diluted solution by inductively coupled plasma – emission spectroscopy (ICP-ES). The Au(III) loadings range from 71.4 mg Au/g nMST to 128.7 mg Au/g, with an average value of 97.3 mg/g. This represents a 33% increase over Au(III) loading on the micron-sized MST, which ranges from 58.0 mg Au/g MST to 88.6 mg/g, with an average value of 73.3 mg/g. TEM images of the nMST after exchange with Au(III) showed the presence of gold with no observable changes in the particle morphology. We believe that Au(III) is incorporated into the lattice of the micron and nanosize MST by coordinating to the oxygen atoms of titania as was observed in previous studies with MST exchanged with Sr^{2+} and UO_2^{2+}.[20]

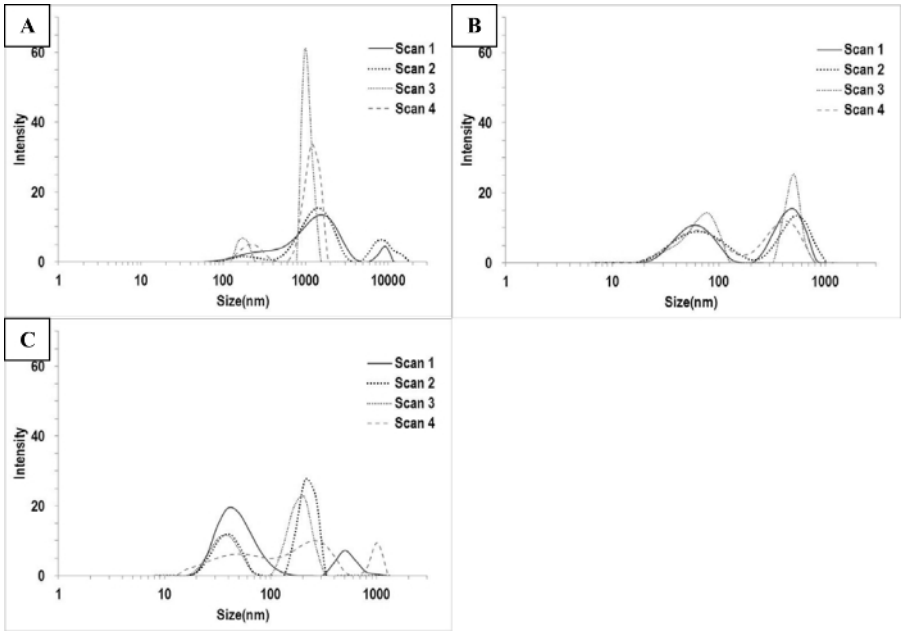

Figure 1. MST and nMST particle size distributions. (**A**) Particle size distribution of MST, (**B**) particle size distribution of nMST synthesized using no surfactant after 24 hr, and (**C**) particle size distribution of nMST synthesized using no surfactant after 48 hr. Reproduced with permission from reference 19. Please click here to view a larger version of this figure.

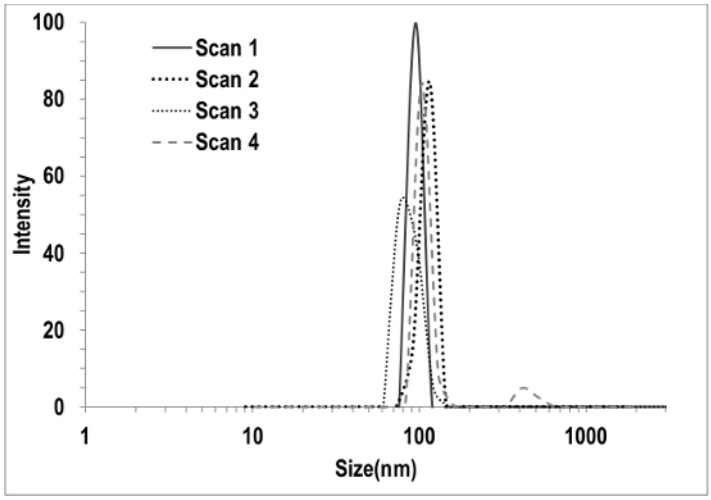

Figure 2. Typical particle size distribution of nMST. Particle size distribution for monosodium titanate synthesized in the presence of Triton X-100. Reproduced with permission from reference 19. Please click here to view a larger version of this figure.

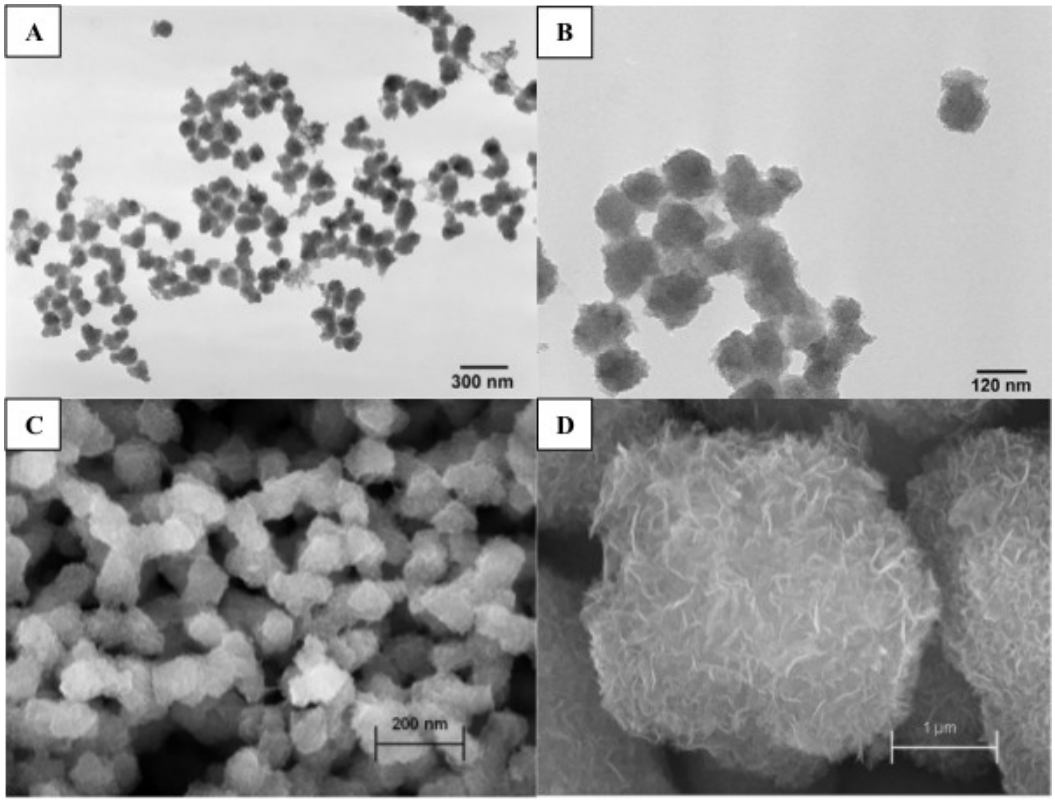

Figure 3. Size and morphology of nMST and MST. (**A**, **B**) Transmission electron microscopy images of nMST; (**C**) scanning electron microscopy image of nMST, and (**D**) scanning electron microscopy image of MST. Reproduced with permission from reference 19. Please click here to view a larger version of this figure.

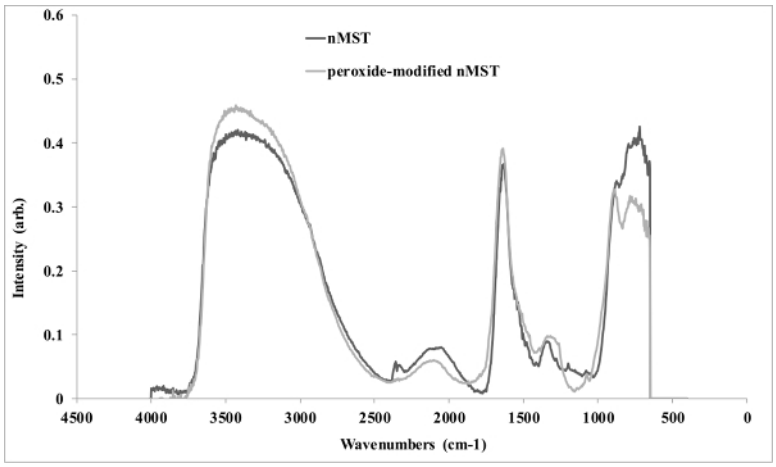

Figure 4. FT-IR absorption spectra of nMST (black) and peroxide-modified nMST (gray). The spectra confirm the formation of the peroxotitanate species as evidenced by the appearance of an absorption band at 883 cm^{-1} for the peroxide-modified nMST. Reproduced with permission from reference 19. Please click here to view a larger version of this figure.

Discussion

The presence of extraneous water, for example from impure reagents, can alter the outcome of the reaction, leading to larger or more polydisperse particles. Therefore, care should be taken to ensure dry reactants are used. The titanium isopropoxide and sodium methoxide should be stored in a desiccator when not in use. High purity isopropanol should also be used for the synthesis.

Temperature was found to play a key role in the conversion of the product from a gel to particulate form. TEM images before and after heating to 82 °C show the product appears as a semi-particulate/semi-gel-like state prior to heating, but after heating the product appears solid and particulate in nature. Thus, the low temperature heating for 45-90 min is needed to complete particulate formation of the nMST.

As noted in this paper, the addition of a surfactant is critical to control the final size of the monosodium titanate. However, for the MST to serve as an effective ion exchanger, the surfactant must be removed so that all sites are accessible for the ion-exchange reaction. Thus, the choice of

a suitable surfactant must consider not only the particle growth properties, but also chemical properties that allow the surfactant to be easily and effectively removed by economical means. In the case of the Triton X series of surfactants, these surfactants are very soluble in water and can be effectively removed by rinsing with water. For other surfactants, effective removal may require rinsing with a non-aqueous liquid.

The technique described in this work has expanded the range of particle sizes of MST that can be prepared, down into the nano regime. This has opened up the possibility for new applications for these materials, including their use as therapeutic metal delivery platforms. The decrease in particle size also increases the sorption kinetics, making the materials more efficient ion-exchangers. Modifications of the conditions used in this technique could further expand the range of particle sizes available, not only to smaller nanomaterials, but also to produce particles of larger size if that is desirable for a particular application.

While this technique is limited to the synthesis of materials that can be prepared using a sol-gel synthesis, it could be applied to other materials beyond MST. Not only could this technique be applied to RT sol-gel syntheses, like the one described, but application to a hydrothermal synthesis could also be envisioned. In the hydrothermal synthesis, the addition of the surfactant to the precursor solution could serve to limit the size of the precursor material formed, leading to faster reaction during the hydrothermal step, and also the possible formation of smaller particles of the final product.

Disclosures

The authors have nothing to disclose.

Acknowledgements

The authors thank the Laboratory Directed Research and Development program at the Savannah River National Laboratory (SRNL) for funding. We thank Dr. Fernando Fondeur for collection and interpretation of the FT-IR spectra and Dr. John Seaman of the Savannah River Ecology Laboratory for the use of the DLS instrument for particle size measurements. We also thank the Dr. Daniel Chan of the University of Washington and the National Institute of Health (Grant #1R01DE021373-01), for funding experiments investigating the ion exchange reactions with Au(III). The Savannah River National Laboratory is operated by Savannah River Nuclear Solutions, LLC for the Department of Energy under contract DE-AC09-08SR22470.

References

1. O'Regan, B., & Grätzel, M. A low-cost, high-efficiency solar cell based on dye-sensitized colloidal TiO_2 films. *Nature.* **353**, 737-740 (1991).
2. Frank, A. J., Kopidakis, N., & van de Lagemaat, J. Electrons in nanostructured TiO_2 solar cells: transport, recombination and photovoltaic properties. *Coord. Chem. Rev.* **248** (13-14), 1165-1179 (2004).
3. Mor, G. K., Varghese, O. K., Paulose, M., Shankar, K., & Grimes, C. A. A review on highly ordered, vertically oriented TiO_2 nanotube arrays: fabrication, material properties, and solar energy applications. *Sol. Energy Mater. Sol. Cells.* **90** (14), 2011-2075 (2006).
4. Dosch, R. G. *Use of titanates in decontamination of defense waste.* Report RS-8232-2/50318. Sandia National Laboratories, Albuquerque, NM (1978).
5. Sylvester, P., & Clearfield, A. The removal of strontium from simulated Hanford tank wastes containing complexants. *Sep. Sci. Technol.* **34** (13), 2539-2551 (1999).
6. Manna, B., Dasgupta, M., & Ghosh, U. C. Crystalline hydrous titanium(IV) oxide (CHTO): an arsenic(III) scavenger from natural water. *J. Water Supply Res. T.*, **53**, 483-495 (2004).
7. Elvington, M. C., Click, D. R., & Hobbs, D. T. Sorption behavior of monosodium titanate and amorphous peroxotitanate materials under weakly acidic conditions. *Sep. Sci. Technol.* **45** (1), 66-72 (2010).
8. Wataha, J. C., *et al.* Titanates deliver metal ions to human monocytes. *J. Mater. Sci.: Mater. Med.* **21** (4), 1289-1295 (2010).
9. Chung, W. O., *et al.* Peroxotitanate- and monosodium metal-titanate compounds as inhibitors of bacterial growth. *J. Biomed. Mater. Res., Part A.* **97** (3), 348-354 (2011).
10. Hobbs, D. T., *et al.* Strontium and actinide separations from high level nuclear waste solutions using monosodium titanate 1. Simulant testing. *Sep. Sci. Technol.* **40** (15), 3093-3111 (2005).
11. Ramirez-Salgdo, J., Djrado, E., & Fabry, P. Synthesis of sodium titanate composites by sol-gel method for use in gas potentiometric sensors. *J. Eur. Ceram. Soc.* **24** (8), 2477-2483 (2004).
12. Yang, J., *et al.* Study on composition, structure and formation process of nanotube $Na_2Ti_2O_4(OH)_2$. *Dalton Trans.* **2003** (20), 3898-3901 (2003).
13. Chen, W., Guo, X., Zhang, S., & Jin, Z. TEM study on the formation mechanism of sodium titanate nanotubes. *J. Nanopart. Res.* **9** (6), 1173-1180 (2007).
14. Meng, X., Wang, D., Liu, J., & Zhang, S. Preparation and characterization of sodium titanate nanowires from brookite nanocrystallites. *Mater. Res. Bull.* **39** (14-15), 2163-2170 (2004).
15. Yada, M., Goto, Y., Uota, M., Torikai, T., & Watari, T. Layered sodium titanate nanofiber and microsphere synthesized from peroxotitanic acid solution. *J. Eur. Ceram. Soc.* **26** (4-5), 673-678 (2006).
16. Stewart, T. A., Nyman, M., & deBoer, M. P. Delaminated titanate and peroxotitanate photocatalysts. *Appl. Catal. B.* **105** (1-2), 69-76 (2011).
17. Rejman, J., Oberle, V., Zuhorn, I. S., & Hoekstra, D. Size-dependent internalization of particles via the pathways of clathrin- and caveolae-mediated endocytosis. *Biochem. J.* **377** (1), 159-169 (2004).
18. Hobbs, D. T., Taylor-Pashow, K. M. L., & Elvington, M. C. *Formation of nanosized metal particles on a titanate carrier.* US Patent Application 14/020,472, Filed Sept. 6 (2013).
19. Elvington, M. C., Tosten, M., Taylor-Pashow, K. M. L., & Hobbs, D. T. Synthesis and characterization of nanosize sodium titanates. *J. Nanopart. Res.* **14**, 1114 (2012).

20. Duff, M. C., Hunter, D. B., Hobbs, D. T., Fink, S. D., Dai, Z., & Bradley, J. P. Mechanisms of strontium and uranium removal from high-level radioactive waste simulant solutions by the sorbent monosodium titanate. *Environ. Sci. Technol.* **38** (19), 5201-5207 (2004).
21. Puangpetch, T., Sreethawong, T., & Chavadej, S. Hydrogen production over metal-loaded mesoporous-assembled $SrTiO_3$ nanocrystal photocatalysts: effects of metal type and loading. *Int. J. Hydrogen Energy.* **35** (13), 6531-6540 (2010).
22. Fan, X., *et al.* Facile method to synthesize mesoporous multimetal oxides ($ATiO_3$, A = Sr, Ba) with large specific surface areas and crystalline pore walls. *Chem. Mater.* **22** (4), 1276-1278 (2010).
23. Rossmanith, R., *et al.* Porous anatase nanoparticles with high specific area prepared by miniemulsion technique. *Chem. Mater.* **20** (18), 5768-5780 (2008).
24. Wu, Y., Zhang, Y., Xu, J., Chen, M., & Wu, L. One-step preparation of PS/TiO_2 nanocomposite particles via miniemulsion polymerization. *J. Colloid Interface Sci*. **343** (1), 18-24 (2010).
25. Jiang, C., Ichihara, M., Honmaa, I., & Zhou, H. Effect of particle dispersion on high rate performance of nano-sized $Li_4Ti_5O_{12}$ anode. *Electrochim. Acta.* **52** (23), 6470-6475 (2007).
26. Bouras, P., Stathatos, E., & Lianos, P. Pure versus metal-ion-doped nanocrystalline titania for photocatalysis. *Appl. Catal. B.* **73** (1-2), 51–59 (2007).
27. Bonino, R., *et al.*, Ti-Peroxo species in the TS-1/H_2O_2/H_2O system. *J. Phys. Chem. B* **108** (11), 3573-3583 (2004).
28. Bordiga, S., *et al.*, Resonance Raman effects in TS-1: the structure of Ti(IV) species and reactivity towards H_2O, NH_3 and H_2O_2: an *in situ* study. *Phys. Chem. Chem. Phys.* **2003** (5), 4390-4393 (2003).
29. Vacque, V., Sombret, B., Huvenne, J. P., Legrand, P., & Suc, S., Characterization of the O-O peroxide band by vibrational spectroscopy. *Spectrochim. Acta Part A.* **53** (1), 55-66 (1997).

